THE JOURNAL OF BIOLOGICAL CHEMISTRY VOL. 290, NO. 9, pp. 5855–5867, February 27, 2015

A Hypertrophic Cardiomyopathy-associated *MYBPC3* Mutation Common in Populations of South Asian Descent Causes Contractile Dysfunction*

Received for publication, September 6, 2014, and in revised form, December 30, 2014 Published, JBC Papers in Press, January 12, 2015, DOI 10.1074/jbc.M114.607911

Diederik W. D. Kuster[‡1], Suresh Govindan[‡], Tzvia I. Springer[§], Jody L. Martin[‡], Natosha L. Finley[§¶], and Sakthivel Sadayappan[‡2]

From the [‡]Department of Cell and Molecular Physiology, Health Sciences Division, Loyola University Chicago, Maywood, Illinois 60153, and the [§]Department of Microbiology and the [¶]Cell, Molecular, and Structural Biology Program, Miami University, Oxford, Ohio 45056

Background: A 25-base pair deletion in the *MYBPC3* gene is the most prevalent hypertrophic cardiomyopathy-associated mutation among South Asian populations.
Results: Expression of mutant protein (cMyBP-C^{C10mut}) in cultured adult rat cardiomyocytes led to improper localization and contractile dysfunction.
Conclusion: cMyBP-C^{C10mut} expression is sufficient to cause contractile dysfunction.
Significance: The study sheds light on the etiology of this ethnic-specific hypertrophic cardiomyopathy mutation.

Hypertrophic cardiomyopathy (HCM) results from mutations in genes encoding sarcomeric proteins, most often *MYBPC3*, which encodes cardiac myosin binding protein-C (cMyBP-C). A recently discovered HCM-associated 25-base pair deletion in *MYBPC3* is inherited in millions worldwide. Although this mutation causes changes in the C10 domain of cMyBP-C (cMyBP-C^{C10mut}), which binds to the light meromyosin (LMM) region of the myosin heavy chain, the underlying molecular mechanism causing HCM is unknown. In this study, adenoviral expression of cMyBP-C^{C10mut} in cultured adult rat cardiomyocytes was used to investigate protein localization and evaluate contractile function and Ca^{2+} transients, compared with wild-type cMyBP-C expression (cMyBP-C^{WT}) and controls. Forty-eight hours after infection, 44% of cMyBP-C^{WT} and 36% of cMyBP-C^{C10mut} protein levels were determined in total lysates, confirming equal expression. Immunofluorescence experiments showed little or no localization of cMyBP-C^{C10mut} to the C-zone, whereas cMyBP-C^{WT} mostly showed C-zone staining, suggesting that cMyBP-C^{C10mut} could not properly integrate in the C-zone of the sarcomere. Subcellular fractionation confirmed that most cMyBP-C^{C10mut} resided in the soluble fraction, with reduced presence in the myofilament fraction. Also, cMyBP-C^{C10mut} displayed significantly reduced fractional shortening, sarcomere shortening, and relaxation velocities, apparently caused by defects in sarcomere function, because Ca^{2+} transients were unaffected. Co-sedimentation and protein cross-linking assays confirmed that C10^{mut} causes the loss of C10 domain interaction with myosin LMM. Protein homology modeling studies showed significant structural perturbation in cMyBP-C^{C10mut}, providing a potential structural basis for the alteration in its mode of interaction with myosin LMM. Therefore, expression of cMyBP-C^{C10mut} protein is sufficient to cause contractile dysfunction *in vitro*.

Hypertrophic cardiomyopathy (HCM)[3] is the most commonly inherited cardiac disease. It is caused by mutations in genes encoding contractile proteins, leading to contractile dysfunction and subsequent hypertrophy. Affected individuals develop pump dysfunction and cardiac hypertrophy at a young age. Moreover, HCM is the most frequent cause of acute cardiac arrest in young people (1). In particular, mutations in the *MYBPC3* gene are responsible for ~40% of all HCM cases (2, 3). *MYBPC3* encodes the thick filament protein cardiac myosin binding protein-C (cMyBP-C). HCM mutations in the *MYBPC3* gene were first identified in 1995 (4, 5), and, to date, ~200 mutations have been published (6). The precise functional and pathological consequences of *MYBPC3* mutations are not fully characterized because mutant proteins are typically not found in cardiac tissue from affected patients (7, 8).

cMyBP-C is a critical regulator of cross-bridge cycling at its N terminus by altering the interaction between myosin, actin, and α-tropomyosin (α-TPM) (9, 10). The C-terminal amino acids of cMyBP-C are responsible for tight binding to the light meromyosin (LMM) region of myosin heavy chain (MyHC), as well as titin (11, 12), which provides sarcomeric stability and anchors cMyBP-C to the sarcomere (Fig. 1*A*). The most important regulatory role of cMyBP-C seems to be its effect on the cross-bridge cycling kinetics of sarcomere contraction (13, 14). It has been proposed that cMyBP-C acts as a structural constraint limit-

* This work was supported, in whole or in part, by National Institutes of Health Grants R01HL105826 and K02HL114749 (to S. S.). This work was also supported by American Heart Association Midwest Affiliate Research Programs Grant-in-Aid 14GRNT20490025 and Postdoctoral Fellowships 13POST17220009 (to D. W. D. K.) and 13POST14720024 (to S. G.).
[1] Present address: Dept. of Physiology, Institute for Cardiovascular Research, VU University Medical Center, Amsterdam, The Netherlands.
[2] To whom correspondence should be addressed: Dept. of Cell and Molecular Physiology, Health Sciences Div., Loyola University of Chicago, 2160 S. First Ave., Maywood, IL 60153. Tel.: 708-216-7994; Fax: 708-216-6308; E-mail: ssadayappan@luc.edu.

[3] The abbreviations used are: HCM, hypertrophic cardiomyopathy; AV, adenoviruses; LMM, light meromyosin; MyHC, myosin heavy chain; α-TPM, α-tropomyosin; MOI, multiplicity of infection; UPS, ubiquitin-proteasome system.

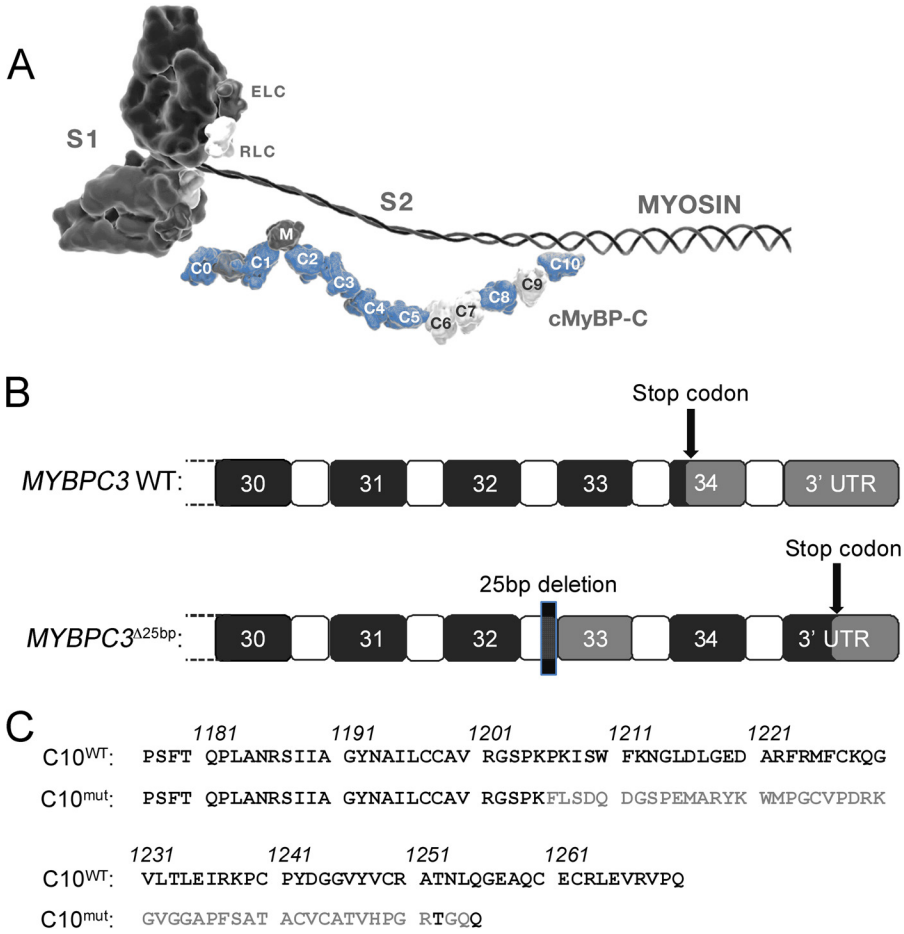

FIGURE 1. **25-base pair deletion in *MYBPC3*.** *A*, schematic representation of the 3′-end of *MYBPC3* gene, showing the coding exons 30–34 (*black*), which contain the stop codon. The HCM-associated 25-base pair deletion in intron 32 leads to skipping of exon 33 and a frameshift. Because the original stop codon is missed by the frameshift, transcription of the entire exon 34 occurs, as well as part of the 3′-UTR. *B*, consequences of *MYBPC3*$^{\Delta 25bp}$ mutation on the protein level include changes in the C10 domain. *C*, in the mouse sequence, the C10 domain consists of amino acids 1177–1270. The *MYBPC3*$^{\Delta 25bp}$ mutation also causes a new sequence of amino acids starting at 1206 and is 15 amino acids shorter than the WT sequence. Only 2 of 50 amino acids are conserved between WT and C10 domain after amino acids 1206.

ing cross-bridge formation and that phosphorylation of cMyBP-C accelerates cross-bridge kinetics, which is required for enhanced rates of relaxation and force development in diastole and systole, respectively (15, 16). cMyBP-C can be phosphorylated by PKA on at least four sites (9) and by glycogen synthase kinase3β (17), in addition to other kinases, such as PKC, PKD, ribosomal S6 kinase, and calcium/calmodulin-dependent kinase II (18).

Among the many hundreds of individual mutations associated with HCM development, a highly prevalent 25-bp deletion mutation was recently discovered in the *MYBPC3* gene (*MYBPC3*$^{\Delta 25bp}$) (19–21). *MYBPC3*$^{\Delta 25bp}$ is estimated to occur in 55 million people worldwide (19). This mutation is pathogenic, because 90% of carriers over 60 years of age have developed HCM (19). Despite its high prevalence, the pathogenic mechanism is completely unknown. The 25-bp deletion leads to the skipping of exon 33 and a frameshift (Fig. 1*B*). The frameshift results in missing the stop codon at the beginning of exon 34, leading to the translation of exon 34, as well as part of the 3′-UTR. In the mouse sequence, this leads to replacement of the last 65 amino acids with a novel sequence of 50 amino acids (cMyBP-C^{C10mut}) (Fig. 1*C*). Despite its pathogenicity and prevalence, the pathophysiological mechanism of this mutation is unknown. Most *MYBPC3* mutations cause haploinsufficiency (8, 22), but cMyBP-C^{C10mut} does not reduce total cMyBP-C levels (19). Therefore, it seems likely that the altered C10 domain is responsible for impairing the function of cMyBP-C by the so-called poison polypeptide effect. Although cMyBP-C^{C10mut} has been associated with cardiomyopathies and an increased risk of heart failure, it is not known whether cMyBP-C^{C10mut} expression alone is sufficient for the development of cardiomyopathy. Therefore, in this study, we aimed to determine *in vitro* whether cMyBP-C^{C10mut} expression is, in fact, sufficient to impair protein stability and localization, thus causing contractile dysfunction in isolated rat cardiomyocytes. Our data did confirm the improper incorporation of cMyBP-C^{C10mut} into the sarcomere by the loss of C10 domain interaction with the LMM region of MyHC. Under these conditions, cMyBP-C^{C10mut} is less able to regulate cardiac contractility, thus providing evidence that HCM is likely caused by the cMyBP-C^{C10mut} protein.

EXPERIMENTAL PROCEDURES

Isolating and Culturing of Adult Rat Cardiomyocytes—This study was conducted in accordance with the Guide for the Care and Use of Laboratory Animals, published by the National

Institutes of Health, using protocols approved by the Institutional Animal Care and Use Committee. Hearts were removed from heparinized and anesthetized adult male Sprague-Dawley rats (aged 3 months with average body weight of 300 g; Harlan Laboratories) and quickly mounted on a Radnotti perfusion apparatus. Cardiomyocytes were isolated as we described before (23). After isolation, Ca^{2+} concentration was increased stepwise to 1.3 mM. Isolated cardiomyocytes were plated on laminin-coated (10 μg/ml in PBS) 6-cm dishes for protein analysis, coverslips for cell shortening and Ca^{2+} transient measurements, or chamber slides for immunofluorescence studies. Isolation buffer was replaced by plating medium (Hanks' minimum essential medium; Invitrogen), 10% (v/v) fetal bovine serum, 10 mM 2,3-butanedione monoxime, and 100 units/ml penicillin/streptomycin). Cells ($\sim 5 \times 10^4$ rod-shaped cells per dish) were plated on dishes and incubated at 95% O_2, 2% CO_2 for 1 h. Plating medium was replaced by culturing medium (Hanks' minimum essential medium, 10 mM 2,3-butanedione monoxime, 2 mM glucose, 0.1% (w/v) BSA, 1× insulin-transferrin-Selenium supplement (Sigma), and 100 units/ml penicillin/streptomycin preincubated at 37 °C, 95% O_2, 2% CO_2 for >1 h). Attached rod-shaped cells were counted with an eyepiece with a cell counting grid. Adenoviruses in multiplicity of infection were added after the cell count. Medium was changed daily, and cells were harvested 48 h after adenovirus infection.

Adenovirus Generation—Adenoviral vectors were generated in pShuttle-CMV utilizing the Stratagene AdEasy XL system (Stratagene, La Jolla, CA). Amplified adenoviruses (AV) were purified via ultracentrifugation through discontinuous cesium chloride gradients before dialysis into 10 mM Tris-HCl, 10 mM $MgCl_2$ at pH 7.4 with 10% glycerol added as a cryopreservative. Titer was estimated by viral particle density at 260 nm (1 OD = 10^{12} particles/ml).

Adenoviral Infection of Smooth Muscle Cells—To create lysates containing 100% cMyc-cMyBP-C, A7r5 smooth muscle cells (ATCC, Manassas, VA) were used. These cells do not express cMyBP-C endogenously. A7r5 cells were plated on 60-mm^2 dishes until 50% confluent and infected with cMyBP-C^{WT}-AV (containing cMyc tag). Cells were cultured for 5 days.

Real Time PCR Analysis—Cultured adult rat ventricular cardiomyocytes were used to extract total mRNA by homogenization, using TRIzol and a Mini-Beadbeater (Biospec). Then chloroform precipitation and purification of total mRNA were performed using an RNA binding column (Bio-Rad 732-6830). Next, cDNA was synthesized using 1 μg of purified total mRNA and an iScript cDNA synthesis kit (Bio-Rad 170-8891). Quantitative PCR was performed with TaqMan primers against *MYBPC3* (IDT Mm.PT.53a.2930640) and with a TaqMan GAPDH primer sequence (Applied Biosystems, Mm00486742m1) as a reference gene. Quantitative PCR and normalized gene expression were calculated as we described previously (22).

Relative Quantification of AV-derived cMyBP-C—Increasing amounts of A7r5 cells + cMyc-cMyBP-C lysate were loaded on a gel, together with lysates from rat cardiomyocytes infected with cMyBP-C^{WT} and cMyBP-C^{C10mut} AV. Proteins were transferred to hybond polyvinylidene difluoride membranes (GE Healthcare Life Sciences). Aspecific binding was blocked by incubating the membranes in SEA Block buffer (Thermo Scientific, Waltham, MA) for 1 h. Membrane was incubated simultaneously with mouse monoclonal antibody against cMyBP-C (E7; Santa Cruz Biotechnology Inc., Dallas, TX) and rabbit polyclonal antibody against cMyc (Roche). Cy3-conjugated anti-mouse IgG and Cy5-conjugated anti-rabbit IgG were used as secondary antibodies. Cy3 and Cy5 fluorescent signals were obtained on a Typhoon 9200 scanner (GE Healthcare Life Sciences). From the increasing amounts of A7r5 + cMyc-cMyBP-C lysates, a standard curve was made for both cMyBP-C (Cy3) and cMyc (Cy5) signals. When within the linear range, the linear regression line will give the following equations.

$$\text{Relative cMyBP-C quantity} = \text{slope} \times (\text{Cy3 signal}) + \text{intercept} \quad \text{(Eq. 1)}$$

$$\text{Relative cMyc quantity} = \text{slope} \times (\text{Cy5 signal}) + \text{intercept} \quad \text{(Eq. 2)}$$

The percentage of AV-derived cMyBP-C (cMyc) in total cMyBP-C (cMyBP-C) in the cardiomyocytes infected with cMyBP-C^{WT} and cMyBP-C^{C10mut} is calculated as (relative quantity cMyc/Relative quantity cMyBP-C) × 100%.

Immunoblotting—Dishes were washed twice with PBS, and cells were harvested in SDS loading buffer. Immunoblotting was performed against cMyBP-C and its phosphorylation level at Ser-273, Ser-282, and Ser-302 sites, cMyc-tag, GAPDH, and α-TPM, as we described previously (24).

Unloaded Shortening and Ca^{2+} Transient Measurements—Forty-eight hours after AV infection with a high AV dose, which led to ~50% mutant protein expression, cells were slowly adapted to Tyrode's solution (135 mM NaCl, 4 mM KCl, 1 mM $CaCl_2$, 1 mM $MgCl_2$, 10 mM glucose, and 10 mM HEPES, pH 7.4). After extensive washing to remove all 2,3-butanedione monoxime, cells were loaded with a Ca^{2+}-sensitive fluorescent dye, Indo-1AM (Invitrogen), for 15 min. Excess dye was removed by washing with Tyrode's solution. Experiments were carried out at room temperature. Cells were electrically paced with pulses of 20V, 4 ms duration at 0.5 Hz. Sarcomere length was measured simultaneously with Ca^{2+} transients, recorded, and analyzed with IonOptix software as we previously described (24).

Subcellular Fractionation of Cultured Cardiomyocytes—Forty-eight hours after AV infection with a high AV dose, which led to ~50% mutant protein expression, cultured cardiomyocytes were harvested in F60 + 1% (v/v) Triton X-100 (100 μl per 35-mm^2 dish). A 25-μl aliquot was taken (total fraction), and the remainder was centrifuged (14,000 × *g*, 5 min, 4 °C). The supernatant was collected (soluble fraction), and the pellet (myofilament fraction) was homogenized in loading buffer.

Immunofluorescence Analysis—Immunofluorescence experiments on cultured adult cardiomyocytes were performed as we described previously (24). Primary antibodies used were mouse monoclonal anti-cMyc (Sigma) and rabbit polyclonal anti-α-actinin, both at a dilution of 1:200, and incubated overnight at 4 °C. Secondary antibody incubations were done with anti-rabbit IgG Alexa 488 and anti-mouse IgG Alexa 568 at a dilution of

1:100 for 1 h at room temperature. Immunofluorescence images were obtained on a Zeiss Axiovert 100 microscope (Carl Zeiss Microimaging, Thornwood, NY).

Recombinant Protein Expression—To generate recombinant protein encoding for human myosin LMM, the gene corresponding to this region was cloned into pET 28a+ with a His-tag. DNA encoding for mouse cardiac C8-C10^{WT} (UniProt accession number O70468; residues 967–1270) and C8-C10^{mut} (residues 967–1256) was subcloned into the pETite vector from the *Expresso*^{TM} SUMO T7 cloning and expression system from Lucigen® according to the manufacturer's protocol. Plasmids were confirmed with DNA sequencing. The C8-C10 plasmids were transformed into *Escherichia coli* HI-Control BL21 (DE3) (Lucigen, Middleton, WI) in accordance with the manufacturer's protocols. Routinely, cells were grown at 37 °C in Luria-Bertani medium containing 30 μg/ml kanamycin and shaken (250 rpm) until optical cell densities (A_{600}) reached 0.8–1.0. Cells were induced with 0.5 mM isopropyl β-D-thiogalactopyranoside and grown at 30 °C. Cells were harvested 20 h postinduction by centrifugation at 4 °C for 30 min at 3700 × *g*. Cell pellets containing recombinant C8-C10^{WT} or C8-C10^{mut} were resuspended in buffer on ice containing 8 M urea, 500 mM NaCl, 10 mM imidazole, 20 mM Tris-HCl, and 1 mM phenylmethanesulfonyl fluoride at pH 8.0. Suspensions were lysed by sonication (FB-705) at 35 mA on ice for 15 s on and 45 s off for a total on time of 3 min. The lysate was centrifuged at 16,000 × *g* for 30 min at 4 °C. Soluble supernatant was loaded onto a 5-ml His-Trap HP Ni-Sepharose resin (GE Healthcare Life Sciences). Proteins were eluted using the same buffer with the addition of 500 mM imidazole. Eluted proteins were dialyzed against buffer at room temperature containing 6 M urea, 150 mM NaCl, 25 mM Tris, and 1 mM PMSF at pH 8.0. Protein concentrations were determined at A_{280} using a NanoDrop spectrometer (Thermo Scientific, Waltham, MA). Molecular extinction coefficients were individually calculated for C8-C10^{WT} and C8-C10^{mut} using the online ExPASy ProtParam tool (25), which is based on the method as described by Gill and von Hippel (26). The molecular extinction coefficient for C8-C10^{WT} was 47900 M^{-1} cm^{-1}, whereas that for C8-C10^{mut} was 46,410 M^{-1} cm^{-1}. Based on these values, both C8-C10^{WT} and C8-C10^{mut} recombinant protein concentrations were calculated and used in the co-sedimentation assay. Protein samples were stored at −20 °C. Both wild-type and C10 mutants were confirmed by Western blot analysis using C10 domain-specific polyclonal antibody and C10^{mut}-specific custom monoclonal antibody (clone ID 8560-1-4M-4K14-1_120915; AbMART, Arlington, MA).

Co-sedimentation Assay—To determine whether C10^{mut} alters C10 domain interaction with the myosin LMM region, a co-sedimentation assay was performed with either C8-C10^{WT} or C8–10^{mut} and myosin LMM 2.7–4 (amino acids 1554–1935) recombinant proteins as described previously by Flashman *et al.* (12). Purified recombinant proteins of C8-C10^{WT} or C8–10^{mut} and myosin LMM recombinant proteins were prespun in a Beckman TLA 100 rotor at 60,000 rpm for 20 min at 4 °C to remove particulates and precipitated proteins and then dialyzed with co-sedimentation buffer (20 mM imidazole, pH 7.4, 180 mM KCl, 1 mM $MgCl_2$, 1 mM EGTA, and 1 mM DTT). Standard curves were generated to convert the intensity ratios of known amounts of recombinant C8-C10 proteins (4–40 pmol) and myosin LMM (40 pmol) in each pellet to molar ratios (mol of C8-C10/mol of myosin LMM; C8-C10/myosin LMM mol/mol ratio). To determine the binding affinity, myosin LMM (5 μM) was then mixed with various concentrations of recombinant C8-C10 proteins (1–30 μM) in Eppendorf tubes in co-sedimentation buffer, followed by incubation at 37 °C for 30 min and centrifugation for 30 min at 100,000 rpm at 4 °C in a TLA100 rotor in an Optima TLX Beckman ultracentrifuge (Beckman Coulter, Fullerton, CA). The supernatant was then removed, and the pellet was washed in the co-sedimentation buffer. The pellet was then redissolved in 20 μl of 2× SDS-PAGE loading buffer (Bio-Rad) and analyzed using SDS-PAGE. The gel was stained in Coomassie Brilliant Blue and imaged on a Chemidoc XRS (Bio-Rad) for protein bands. The image files (TIFF format) were then used to quantify the band intensities using ImageJ (National Institutes of Health, Bethesda, MD). Following the assay, bound C8-C10 was determined by comparing the band intensity ratios from each pellet fraction to the corresponding molar ratios provided in the standard curve. Saturation binding curves were generated by plotting the bound C8-C10 molar ratios *versus* the total C8-C10 concentrations added using the one-site binding (hyperbola) feature with a nonlinear regression curve fit in GraphPad Prism version 6.00 for Mac OS X (GraphPad Software, San Diego, CA). The maximum molar binding ratio (B_{max}) and dissociation constant (K_d) for each assay were then determined as previously described by Shaffer *et al.* (27).

Cross-linking Studies—To verify co-sedimentation results, cross-linking studies were performed to determine whether C10^{mut} alters C10 interaction with myosin LMM region as described previously by Dihazi and Sinz (28). 6 μM of recombinant proteins encoding C8–10^{WT} and C8-C10^{mut} of cMyBP-C and myosin LMM regions were used in a 400-μl reaction with 60 μM (10-fold) of the cross-linking reagent bis[sulfosuccinimidyl] suberate (Thermo Fisher Scientific, Inc., Rockford, IL) and 20 mM HEPES buffer, pH 7.7. The reaction was incubated at room temperature for 60 min and terminated by adding 5 μl of 50 mM Tris, pH 7.5. A control reaction without cross-linking reagent was prepared in the same manner without bis[sulfosuccinimidyl] suberate. The reaction samples were then run on SDS-PAGE, and the results were analyzed.

Homology Modeling—Tertiary structure prediction for C10^{WT} and C10^{mut} was accomplished using SWISS-MODEL Workspace (29, 30). The primary amino acid sequences of C10^{WT} and C10^{mut} were used as targets, and multiple template structures were identified. The top scoring homology models were selected for C10^{WT} and C10^{mut}. Model quality was assessed using QMEAN4 (31) scores, and each homology model was further subjected to PROCHECK analysis using the PDBsum server (32).

Statistical Analysis—Statistical analysis was performed using GraphPad Prism (version 6). Statistical difference between groups was first determined using one-way analysis of variance, followed by Tukey's post hoc test. A p value <0.05 was considered to be statistically significant.

RESULTS

Adenoviral-induced Expression of cMyBP-C^{C10mut} in Adult Rat Cardiomyocytes—To express cMyBP-C^{C10mut} in adult rat cardiomyocytes, AV infection was used in the present study. Cultured cardiomyocytes were infected with different levels of multiplicity of infection (MOI) of AV encoding cMyc-tagged cMyBP-C^{WT} or cMyBP-C^{C10mut} complementary DNA. To determine whether cMyBP-C transcript levels were increased in a MOI-dependent manner after 48 h of AV infection, real time PCR was performed to determine total transcript levels of cMyBP-C, followed by normalization with the expression level of housekeeping gene GAPDH. As expected, a significant increase in total cMyBP-C transcripts was achieved after 48 h of AV transduction (Fig. 2*A*). Next, profiles of total protein lysates were determined by SDS-PAGE, followed by SYPRO staining. Results showed that no gross changes were observed in overall protein expression after AV transduction (Fig. 2*B*). However, Western blot analyses with antibody against cMyc-tag revealed that an AV dose-dependent increase in expression of cMyBP-C^{WT} and cMyBP-C^{C10mut} exogenous proteins was seen (Fig. 2*C*). Quantitative data revealed that similar expression levels of exogenous cMyBP-C^{WT} or cMyBP-C^{C10mut} could be achieved 48 h postinfection (Fig. 2*D*). Viral expression of cMyBP-C^{WT} seemed to lead to replacement of endogenous cMyBP-C, rather than addition, because total cMyBP-C levels were unchanged after AV infection, whereas in cMyBP-C^{C10mut}, at last partial addition was observed because total cMyBP-C levels increased at high MOI (Fig. 2*E*).

Quantification of cMyBP-C^{C10mut} Expression—The mass difference between cMyBP-C^{C10mut} and endogenous cMyBP-C was too small to resolve on SDS-PAGE (cMyBP-C^{WT}: 140,632 Da; cMyBP-C^{C10mut}: 138,466 Da). Therefore, quantification of the amount of expression of the AV-derived cMyBP-C^{C10mut} was performed using a standard series (Fig. 3). The cMyc-tagged cMyBP-C^{WT} was expressed in rat A7r5 smooth muscle cells, which had no endogenous cMyBP-C expression. Increasing amounts of these lysates were applied to a gel together with AV-infected cardiomyocytes. Subsequently, the amount of cMyBP-C (endogenous + AV-derived protein) and cMyc (only AV-derived protein) was measured with dual color fluorescent immunoblotting (Fig. 3*A*). Slopes of the cMyBP-C and cMyc standard series were used to calculate the percentage of cMyc-tagged cMyBP-C in total cMyBP-C (Fig. 3*B*). After 48 h of infection, AV-virus-derived cMyBP-C^{WT} made up 44 ± 13% of total cMyBP-C, and cMyBP-C^{C10mut} accounted for 36 ± 10% of total cMyBP-C (Fig. 3*C*).

Mislocalization of cMyBP-C^{C10mut} in the Sarcomere—To assess whether AV-derived exogenous cMyBP-C^{WT} and cMyBP-C^{C10mut} proteins properly localized in the C-zone of the sarcomere, immunofluorescence staining was performed using rabbit polyclonal antibodies against N′-region of cMyBP-C and monoclonal antibody against cMyc, followed by confocal microscopy. Co-localization was determined by line scans using ImageJ software (National Institute of Health). Results show that expression of AV-derived cMyBP-C^{WT} protein properly localized in the C-zone by the appearance of two distinct bands (doublets) between Z-lines, as visualized by α-actinin staining (Fig. 4, *A* and *C*), representing a characteristic localization pattern of cMyBP-C. Staining with cMyBP-C antibody, which recognizes both endogenous cMyBP-C and AV-derived cMyBP-C^{WT} exogenous, showed exact co-localization with cMyc staining in the cMyBP-C^{WT}-infected cells (Fig. 4, *B* and *D*), confirming that cMyc-tagged exogenous cMyBP-C^{WT} protein properly localized in the C-zone of the sarcomere. In contrast, cMyBP-C^{C10mut} localization was characterized by the

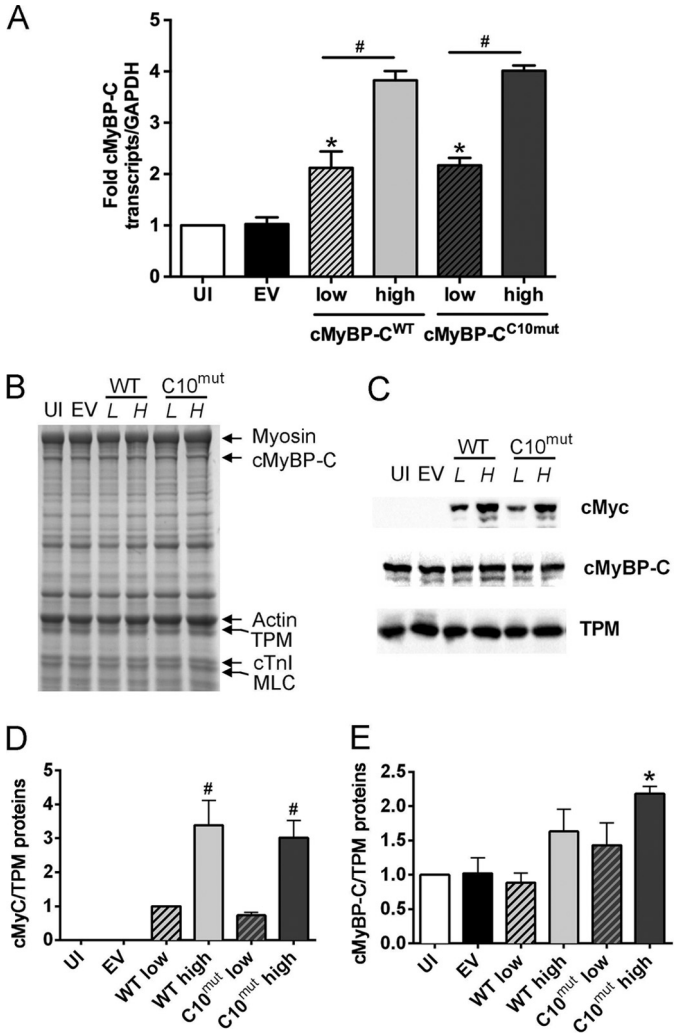

FIGURE 2. **Adenoviral expression of cMyBP-C^{C10mut} in cultured isolated rat cardiomyocytes.** Isolated rat cardiomyocytes were cultured without infection (uninfected, *UI*), with adenovirus and without protein coding sequence (empty vector, *EV*), with cMyBP-C^{WT}, or with cMyBP-C^{C10mut}. Adenovirus-derived cMyBP-C (WT and C10^{mut}) are N-terminally cMyc-tagged to distinguish AV-derived cMyBP-C from endogenous cMyBP-C. Low (*L*) and high (*H*) MOI of cMyBP-C^{WT} and cMyBP-C^{C10mut} were used to achieve dose-dependent protein expression. Cells were harvested 48 h postinfection. *A*, transcript levels of cMyBP-C relative to GAPDH expression and UI controls show a significant increase in cMyBP-C transcripts in a MOI-dependent manner. *B*, representative Coomassie-stained gel of total lysates of cultured cardiomyocytes show no apparent differences in overall protein levels. *C*, immunoblotting for cMyc (virus-derived cMyBP-C), cMyBP-C (endogenous + virus-derived cMyBP-C), and α-TPM as a loading control. *D*, quantification of cMyc levels, showing that similar levels of cMyBP-C^{WT} and cMyBP-C^{C10mut} were expressed 48 h postinfection. *E*, quantification of cMyBP-C levels, normalized with the levels of α-TPM, showed no significant increases in total cMyBP-C levels except cMyBP-C^{C10mut} high MOI expression. The data in *A*, *C*, and *D* were averages ± S.E. from three independent experiments. *, $p < 0.01$ *versus* empty vector/uninfected; #, $p < 0.01$ *versus* respective low MOI virus titers ($n = 4–6$).

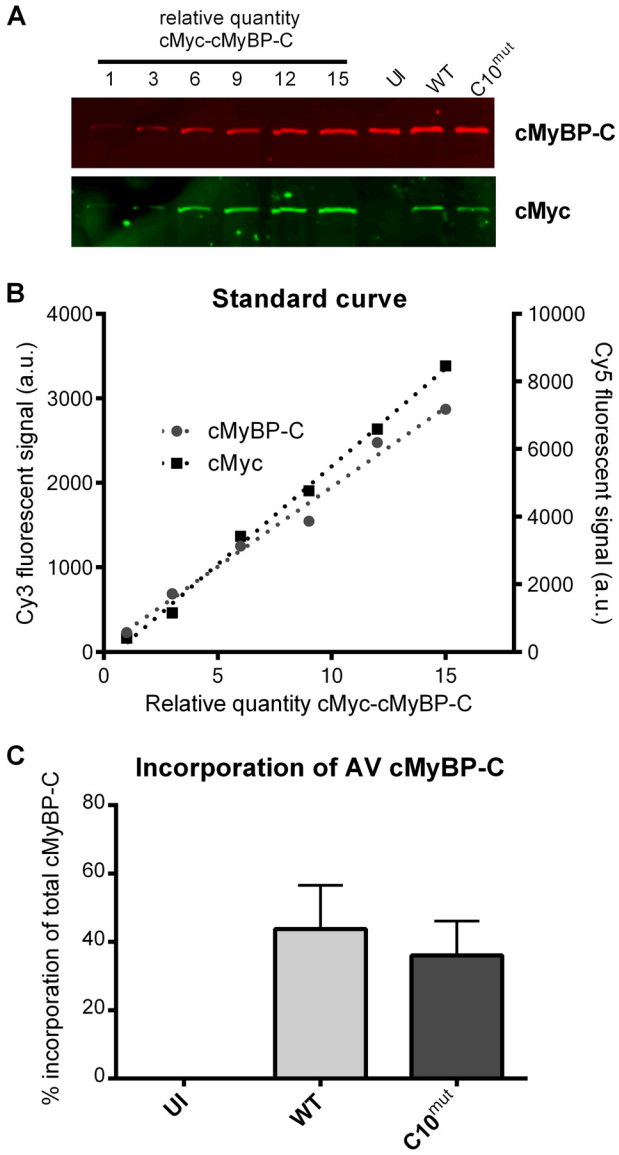

FIGURE 3. **Relative quantification of AV-derived cMyBP-C.** *A*, A7r5 smooth muscle cells with no endogenous cMyBP-C were infected with cMyBP-C^{WT}-AV. A7R5 cell lysates were loaded in different amounts on gel, as well as cultured cardiomyocytes infected with cMyBP-C^{WT} or cMyBP-C^{C10mut}. After transfer, membranes were simultaneously incubated with cMyc (rabbit polyclonal) and cMyBP-C (mouse monoclonal) antibodies. Cy3-labeled anti-mouse IgG and Cy5-labeled anti-rabbit IgG secondary antibodies were used to measure total cMyBP-C (endogenous + virus-derived) and cMyc (virus-derived). *B*, Cy3 and Cy5 samples from A7r5 samples loaded in different amounts were used to make a standard curve. These signals were used to calculate percentages of virus-derived (cMyc) signal to total cMyBP-C (cMyBP-C). *C*, standard curve was used to calculate percentage of virus-derived cMyBP-C to total cMyBP-C present in total lysates 48 h postinfection without virus (uninfected, *UI*), with cMyBP-C^{WT}-AV or with cMyBP-C^{C10mut}-AV. The data are presented as means ± S.E. of three independent experiments.

absence of doublet patterns between Z-lines with either cMyBP-C or cMyc antibody. Furthermore, cMyc staining of cMyBP-C^{C10mut} showed co-localization with α-actinin at the Z-line (Fig. 4, *A*, indicated with *arrows*, and *C*), which is an unusual localization pattern. Co-staining of cMyBP-C^{C10mut} protein with cMyBP-C and cMyc antibodies showed only limited overlap in the C-zone (Fig. 4, *B* and *D*), confirming minimal localization of cMyBP-C^{C10mut} in the C-zone of the sarcomere and more mislocalization to the Z-line in the sarcomere. Because cMyBP-C^{C10mut} is mislocalized more in the Z-line, these data indicate that cMyBP-C^{C10mut} targeting may contribute to the contractile dysfunction.

Subcellular Localization of cMyBP-C^{C10mut}: Subcellular Fractionation—To quantify the amount of cMyBP-C^{C10mut} that localizes to the myofilament fraction, subcellular fractionation of the cultured cardiomyocytes was performed. Cardiomyocyte lysates (total fraction) were separated into detergent-soluble fraction (mainly cytosolic fraction) and myofilament fraction (Fig. 5*A*). Fractionation was shown to be successful with GAPDH (cytosolic marker) and α-TPM (myofilament marker) exclusively present in the expected fractions (Fig. 5*B*). In uninfected cardiomyocytes and cardiomyocytes infected with EV, no cMyBP-C was seen in the soluble fraction (Fig. 5*C*). In contrast, cMyBP-C was observed in the soluble fraction in the cMyBP-C^{WT}-infected cells and especially cMyBP-C^{C10mut}-infected cells (Fig. 5*C*). The higher level of soluble cMyBP-C in the cMyBP-C^{C10mut} AV cells compared with cMyBP-C^{WT} AV cells resulted from reduced incorporation of cMyBP-C^{C10mut} into the sarcomere (Fig. 5, *C* and *D*), as illustrated by the reduced cMyc signal.

Effect of cMyBP-C^{C10mut} Expression on Unloaded Shortening and Ca^{2+} transients of Isolated Cardiomyocytes—For functional analysis of the effect of cMyBP-C^{C10mut}, unloaded shortening experiments were performed in cultured cardiomyocytes. Two days after AV infection, cells were loaded with the Ca^{2+}-sensitive fluorophore indo1-AM, and both cell shortening and Ca^{2+} transients were measured in cells stimulated at 0.5 Hz (Fig. 6*A*). cMyBP-C^{C10mut} expression significantly reduced contractility (Fig. 6, *B* and *C*), velocity of shortening (Fig. 6*D*), and relaxation (Fig. 6*E*). These changes in contractility were not explained by changes in calcium handling (Fig. 7*A*), because neither calcium transient amplitude (Fig. 7*B*) nor calcium transient decay (Fig. 7*C*) was changed. Similar results for sarcomere shortening and Ca^{2+} transients were obtained when cells were paced at 1 Hz (data not shown). Next, to determine whether expression of cMyBP-C^{C10mut} alters total phosphorylation levels of cMyBP-C at Ser-273, Ser-282, and Ser-302, Western blot analyses were performed using phospho-specific antibodies. The results showed that the total cMyBP-C phosphorylation level at Ser-273, Ser-282, and Ser-302 was not significantly altered by the expression of cMyBP-C^{C10mut} compared with control groups (Fig. 7*D*). Taken together, these data suggest that expression of cMyBP-C^{C10mut} in adult rat cardiomyocytes *in vitro* is sufficient to cause contractile dysfunction without affecting Ca^{2+} transients or phosphorylation status.

cMyBP-C^{C10mut} Failed to Interact with LMM Region of MyHC—Previous studies determined that the C10 domain of cMyBP-C interacts with the myosin LMM region (12), which is necessary for cMyBP-C stability in the sarcomere. In the present study, we hypothesized that cMyBP-C^{C10mut} has lost its ability to interact with the myosin LMM region. To test this hypothesis, three recombinant proteins, including C8-$C10^{WT}$, C8-$C10^{mut}$, and myosin LMM, were generated and purified by the Ni-NTA-agarose system (Fig. 8*A*). Both C8-$C10^{WT}$ and C8-$C10^{mut}$ were confirmed by Western blot analyses using $C10^{WT}$- and $C10^{mut}$-specific antibodies (Fig. 8*B*). Then a co-sedimentation assay was performed using either recombinant

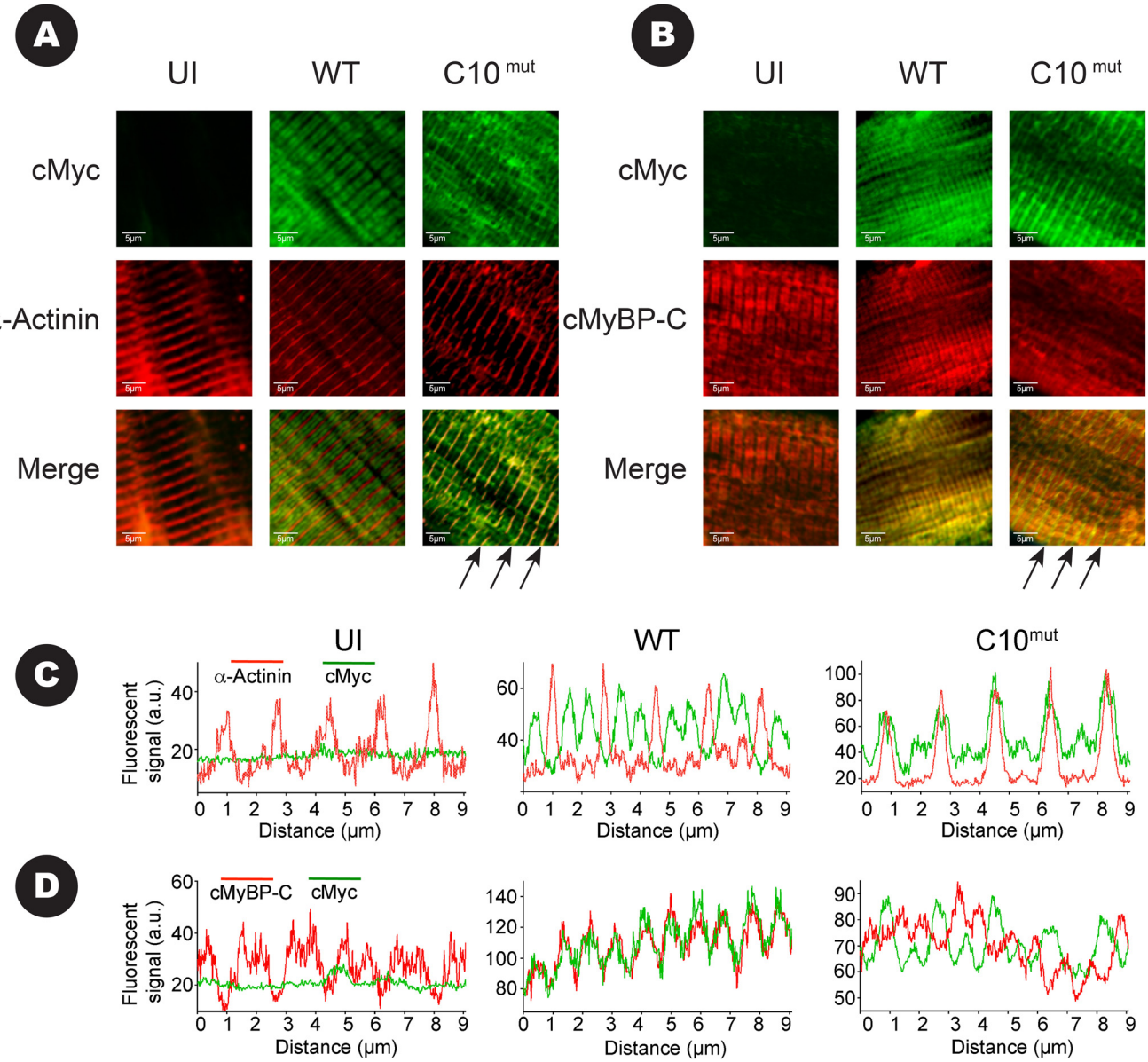

FIGURE 4. **Determination of localization of AV-derived cMyBP-C with immunofluorescence.** Cultured rat cardiomyocytes infected for 48 h with cMyBP-C^{WT}, cMyBP-C^{C10mut}, or uninfected (*UI*). *A*, cells were stained for cMyc (*green*) and α-actinin (*red*) so that co-localization of signal would give a *yellow signal* in the merged images. In cells infected with cMyBP-C^{WT}, the classical staining pattern of two cMyBP-C bands between Z-lines (stained with α-actinin) was seen, indicating proper localization of AV-virus-derived cMyBP-C^{WT}. In uninfected cells, no nonspecific cMyc signal was detected. In cells infected with AV-expressing cMyBP-C^{C10mut}, co-localization of cMyc and α-actinin signal was observed (*arrows*), with only minor signal between Z-lines. *B*, cells were stained for cMyc (*green*) and cMyBP-C (*red*). Note that the cMyBP-C antibody will bind to endogenous cMyBP-C, as well as AV-derived cMyBP-C^{WT} and cMyBP-C^{C10mut}. In UI and cMyBP-C^{WT}, cMyBP-C signal showed doublet staining, with no staining in the Z-lines. cMyBP-C signal in cMyBP-C^{C10mut}-infected cells showed the two cMyBP-C bands, with additional staining in the Z-line. Merging of the cMyc signal and the cMyBP-C signal mainly showed co-localization in the Z-line (*arrows*), with almost no overlaps in the C-zones. *C*, fluorescent line scans of figures in *A* show that cMyBP-C^{WT} (*green*) forms a doublet between two Z-lines (*red*), as is expected for cMyBP-C. In contrast, cMyBP-C^{C10mut} (*green*) only shows overlap within the Z-line marker α-actinin (*red*). *D*, fluorescent line scans of figures in *B* show that cMyBP-C^{WT} (*green*, stained with cMyc) overlaps completely with total cMyBP-C (*red*, stains both endogenous and AV-derived cMyBP-C). In contrast, cMyBP-C^{C10mut} (*green*) shows only minor overlap with endogenous cMyBP-C (*red*).

proteins of C8-$C10^{WT}$ or C8-$C10^{mut}$ with myosin LMM recombinant proteins. Results showed that C8-$C10^{WT}$, but not C8-$C10^{mut}$, interacts with myosin LMM protein (Fig. 8, *C–E*). Furthermore, a dose-dependent interaction was determined using C8-$C10^{WT}$ recombinant proteins with a dissociation constant (K_d) of 9.8 ± 1.8 μM and a molar binding ratio (B_{max}) of 1.14 ± 0.08 (Fig. 8, *F* and *G*). In agreement with previous studies (12), our results showed that C8-$C10^{WT}$ strongly interacts with the myosin LMM region at 1:1 (mol/mol) equimolar concentration. In contrast, the presence of $C10^{mut}$ caused the loss of C8-$C10^{mut}$ interaction with myosin LMM (Fig. 8*G*); therefore, no binding affinities could be determined, suggesting a possible mechanism for the development of HCM disease through impaired sarcomere anchoring. To validate these results, a cross-linking assay was carried out with bis[sulfosuccinimidyl] suberate cross-linking agent, and the products were resolved on a 12% SDS-PAGE (Fig. 8*H*). As expected, C8-$C10^{WT}$ protein interacted with myosin LMM and showed an upper band of ~75 kDa in a position, which is absent in the cMyBP-C^{C10mut} reaction,

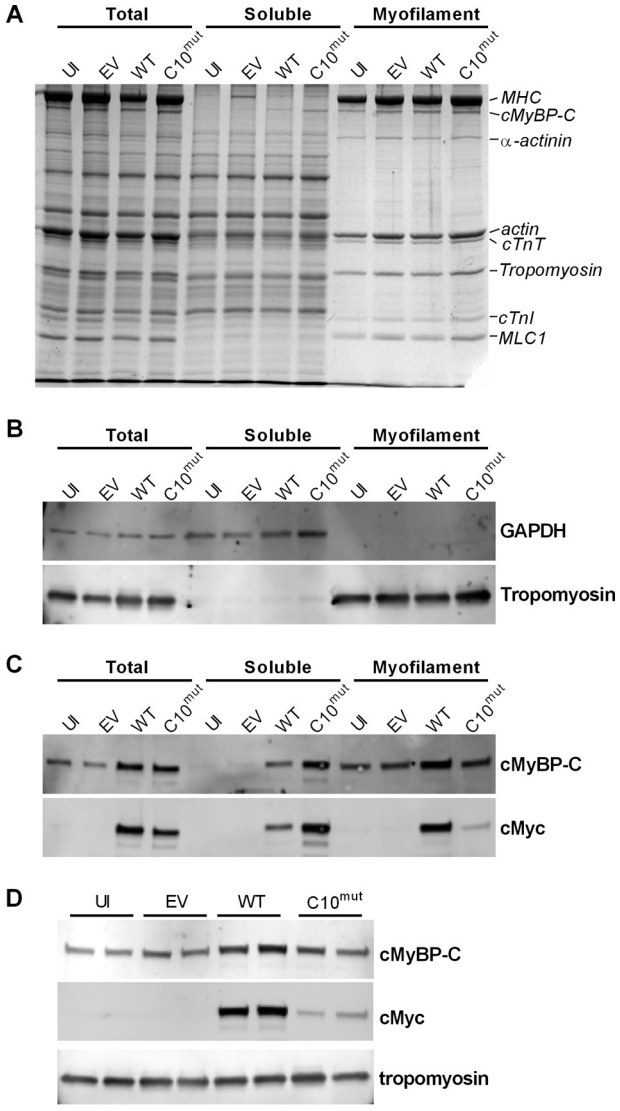

FIGURE 5. **Determination of localization of AV-derived cMyBP-C with subcellular fractionation.** Cultured cardiomyocytes were homogenized in buffer containing 1% Triton X-100 and centrifuged. Supernatant was named soluble, whereas the pellet was named myofilament fraction. *A*, Coomassie-stained SDS-polyacrylamide gel of total, soluble, and myofilament fractions. *B*, high fractionation efficiency was achieved as shown by using markers for cytosol (GAPDH) and myofilament (α-TPM). *C*, dual color immunoblots incubated with antibodies against cMyBP-C (endogenous + virus-derived cMyBP-C) and cMyc (virus-derived cMyBP-C). No cMyBP-C was detected in soluble fraction of uninfected (*UI*) or empty vector (*EV*) fractions, whereas it was detected in cMyBP-C^{WT} and, especially, in cMyBP-C^{C10mut}. cMyc signal shows the lower incorporation of cMyBP-C^{C10mut} into the sarcomere. *D*, immunoblots of myofilament fractions of UI, EV, cMyBP-C^{WT}, and cMyBP-C^{C10mut} cells showed that cMyBP-C^{C10mut} incorporated into the sarcomere at a lower level than cMyBP-C^{WT}.

confirming that cMyBP-C^{C10mut} has completely lost C10 domain interaction with myosin LMM.

$C10^{WT}$ and $C10^{mut}$ Tertiary Structure Analyses Using Homology Modeling—No high resolution structures are available for cMyBP-C or the C10 domain. Therefore, protein homology modeling using SWISS-MODEL Workspace was used to predict the tertiary structures of $C10^{WT}$ and $C10^{mut}$. Template sequences (Protein Data Bank codes 1U2H and 2J8H) were identified for $C10^{WT}$ and $C10^{mut}$, respectively. Each template selected for modeling had a minimum of 28% sequence identity to and 58% sequence coverage for the C10 domain. In the $C10^{mut}$ model, the C-terminal portion was built in as a loop because this region had lower sequence coverage with the selected templates as compared with $C10^{WT}$. Valid models of $C10^{WT}$ and $C10^{mut}$ were determined by QMEAN4 and PROCHECK analyses, and top scoring models were selected as representative structures. Both $C10^{WT}$ and $C10^{mut}$ models had >90% of residues in the most favorable regions as indicated by PROCHECK analyses. Based on the secondary structure content visible in each model, $C10^{WT}$ largely consisted of β-sheet secondary structure (Fig. 9*A*). In direct contrast, $C10^{mut}$ exhibited a marked reduction in β-sheet composition (Fig. 9*B*). Additionally, the $C10^{WT}$ model exhibited a well folded global structure, whereas $C10^{mut}$ was less structurally defined, particularly in the C-terminal region.

DISCUSSION

The outcomes of this study showed that the expression of cMyBP-C^{C10mut} is sufficient to cause contractile impairment in isolated rat cardiomyocytes *in vitro*. This reduced contractility was caused by impaired myofilament function, because no differences were observed in amplitude and kinetics of Ca^{2+} transients. Improper localization of cMyBP-C^{C10mut} occurs, as illustrated by 1) reduced incorporation in the myofilament fraction, 2) predominant Z-disc localization *versus* wild-type localization to the C-zone, and 3) loss of cMyBP-C^{C10mut} interaction with the myosin LMM region. These data suggest that cMyBP-C^{C10mut} localizes improperly in the sarcomere and may bind to other sarcomeric proteins, thus acting as a "poison polypeptide" to reduce contractility.

cMyBP-C^{C10mut} Fails to Incorporate into the Sarcomere—The 25-bp deletion in intron 32 of *MYBPC3* leads to skipping of exon 33 and a frameshift. The consequences of this mutation on the protein level are changes in most residues of the C-terminal domain, *i.e.* the C10 domain. For correct incorporation into the C-zone of the sarcomere, domains C7–C10 are important, with domain C10 being vital for incorporation (33). This localization is mediated through interactions with the LMM region of MyHC (11, 34) and titin (35, 36). The interaction between titin C-zone immunoglobulin domains and MyBP-C occurs within domains C8-C10 (35). The LMM of MyHC makes up the rod region of the thick filament, and interaction with cMyBP-C occurs through the C10 domain of cMyBP-C (34, 37, 38). Specifically, a set of five charged amino acids were identified to be responsible for LMM binding (34). On LMM, the region stretching from amino acids 1554 to 1581 was found to be the binding domain of C10 (12). Based on the predicted LMM-binding region and the structural insights derived from homology modeling studies for the C10 domain, the tertiary structure altered by cMyBP-C^{C10mut} could be expected to reduce affinity for LMM. Of the five identified amino acids necessary for LMM binding (34), only Arg-1201 remains unchanged in cMyBP-C^{C10mut}. Asp-1216, Asp-1220, Arg-1237, and Lys-1238 are all changed. The negatively charged Asp-1216 and Asp-1220 are changed to uncharged methionine and the positively charged lysine, respectively, whereas the positively charged Arg-1237 and Lys-1238 are changed to the uncharged phenylalanine and serine. In our homology models, the LMM-binding surface was

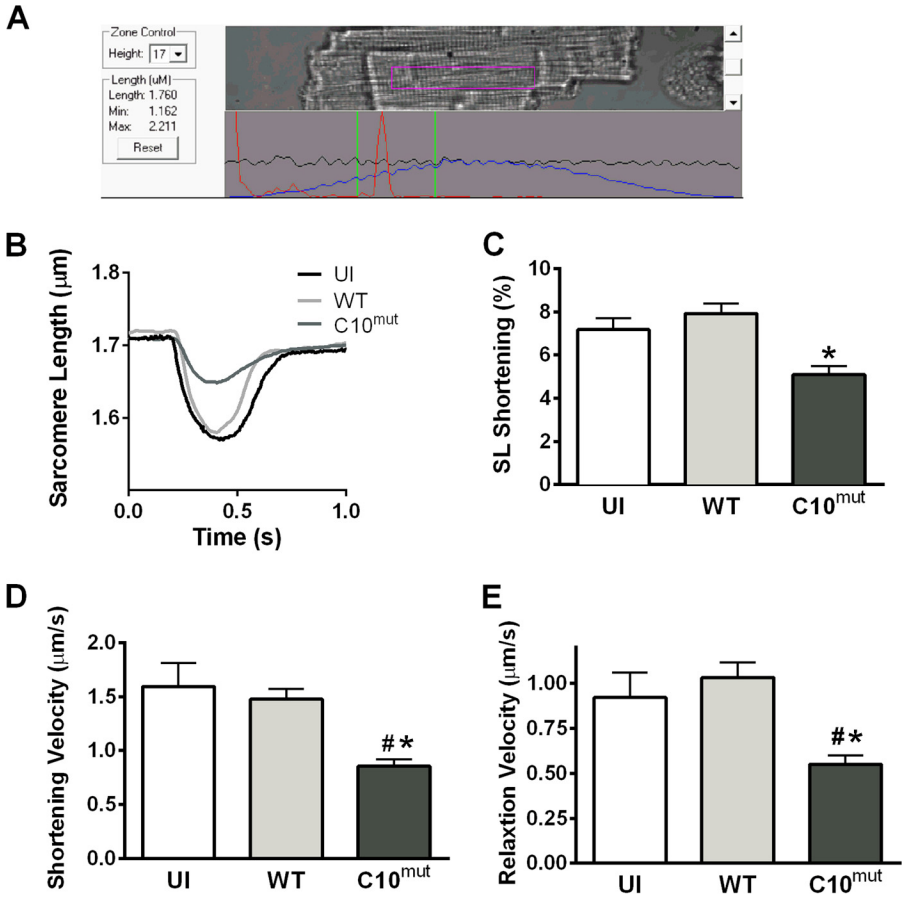

FIGURE 6. **Contractile function after cMyBP-C^{C10mut} expression.** Isolated rat cardiomyocytes were uninfected (UI) or infected with either cMyBP-C^{WT} or cMyBP-C^{C10mut} and cultured for 48 h. Unloaded shortening was measured in these cells. *A*, example of isolated rat cardiomyocyte in which sarcomere length and Ca^{2+} transients were measured simultaneously. *B* and *C*, fractional shortening was reduced in cMyBP-C^{C10mut}-infected cells, compared with uninfected or cMyBP-C^{WT}-expressing cells. *D* and *E*, the kinetics of contraction was also disturbed after cMyBP-C^{C10mut} expression, with slower shortening velocity (*D*) and relaxation velocity (*E*) compared with uninfected cells and cMyBP-C^{WT}. The data are means ± S.E. of four independent experiments. #, $p < 0.05$ in cMyBP-C^{C10mut} *versus* uninfected; *, $p < 0.05$ in cMyBP-C^{C10mut} *versus* cMyBP-C^{WT}.

diminished, and the global fold was destabilized in C10^{mut} as compared with C10^{WT}. Therefore, we proposed that cMyBP-C^{C10mut} alters the incorporation of cMyBP-C into the sarcomere. Transgenic expression of a cMyc-tagged cMyBP-C in mouse hearts does not result in any aberrant phenotype and does not affect the overall stoichiometry of cMyBP-C or other sarcomeric proteins (39). Similarly, although cMyBP-C^{WT} transcripts were increased in a MOI-dependent manner, total cMyBP-C^{WT} protein levels in the cardiomyocytes were unchanged *in vitro*, suggesting that cMyBP-C stoichiometry was maintained by the overexpression of cMyBP-C^{WT} transcripts using AV. In contrast, cMyBP-C^{C10mut} protein levels were significantly increased in the cardiomyocytes, indicating that cMyBP-C^{C10mut} protein incorporation and regulatory pathways were altered by cMyBP-C^{C10mut}. To further support these findings, cMyBP-C^{C10mut} levels in the myofilament fraction were found to be much lower than those of cMyBP-C^{WT}, and levels of cMyBP-C^{C10mut} were higher in the cytoplasm. Moreover, cMyBP-C^{C10mut} only had minor C-zone staining and appeared more at the Z-disc (Fig. 4, *A* and *C*), indicating a lack of C-terminal interaction with myosin LMM, leading, in turn, to the differential localization of cMyBP-C^{C10mut} in the sarcomere. However, it is unknown whether this Z-line localization has direct functional implications. Interestingly, cross-linking and co-sedimentation experiments confirm that cMyBP-C^{C10mut} failed to interact with the LMM region *in vitro*. Taken together, then, cMyBP-C^{C10mut} mutation causes sufficient structural changes in the C10 domain to reduce its affinity for LMM and prevent proper localization of the protein. Partial incorporation of cMyBP-C^{C10mut} full-length protein through its N-terminal region in the sarcomere fraction may result from its interaction with other proteins.

cMyBP-C^{C10mut} Is Sufficient to Cause Contractile Dysfunction in Vitro—Approximately 40% of identified HCM mutations are in *MYBPC3* (2, 3), of which 70% are either truncation or frameshift mutations, making it the most common cause of HCM. To date, ~200 individual mutations in *MYBPC3* have been identified, with the prevalence of individual mutations being low (6). Notable exceptions to this limited distribution of individual mutations can be found, including, for example, the 2373insG founder mutation, which is responsible for almost 25% of all HCM mutations in The Netherlands (40), or the recently described c.927–2A>G founder mutation that occurs in almost 60% of Icelandic HCM patients (41). However, the most prevalent HCM-associated mutation is the 25-bp deletion mutation, which is estimated to occur in 55 million people worldwide (19). This deletion mutation was first identified in 2003 (21) and occurs almost exclusively in South Asian popu-

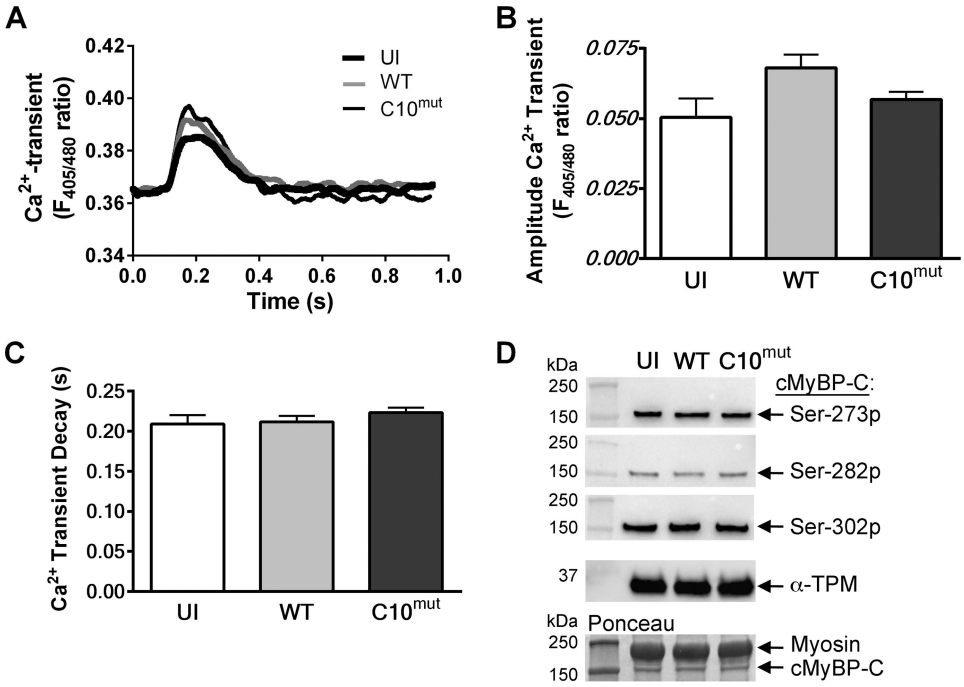

FIGURE 7. **Calcium transients and cMyBP-C phosphorylation levels in cultured cardiomyocytes.** Concomitant with unloaded shortening, Ca^{2+} transients were measured. Cells were loaded with the Ca^{2+}-sensitive fluorescent dye Indo-1. Ca^{2+} release into the cytosol was determined by measuring the ratio between Ca^{2+}-bound Indo signal (at 405 nm) and Ca^{2+}-unbound Indo signal (at 480 nm). *A*, representative traces of Ca^{2+} transients of uninfected (*UI*), cMyBP-C^{WT}- and cMyBP-C^{C10mut}-infected cells. *B*, no changes were seen in amplitude of the Ca^{2+} transient. *C*, Ca^{2+} reuptake kinetics (displayed as tau) was also unaffected by cMyBP-C^{C10mut} expression. The data are means ± S.E. of four independent experiments. *D*, representative Western blot analyses of cMyBP-C phosphorylation at Ser-273 (Ser-273p), Ser-282 (Ser-282p), and Ser-302 (Ser-302p) sites using phospho-specific antibodies. cMyBP-C levels, as measured by Ponceau S staining, and α-TPM levels, as assessed by Western blot, were used as loading controls. 10 μg of total cultured cardiomyocyte lysate was used to perform the Western blot analyses. Quantitative data showed no significant difference among all the groups (data not shown).

lations (19, 42). Previous studies have only shown an association between the *MYBPC3* 25-bp deletion and cardiomyopathies. In the present study, we show that expression of cMyBP-C^{C10mut} in isolated cardiomyocytes from healthy rats is enough to cause contractile dysfunction. The contractile dysfunction could not be explained by changes in Ca^{2+} transients; therefore, such dysfunction likely results from direct impairment of sarcomeric function. Even though the C10 domain mutation prevents proper anchoring in the C-zone of the mutant protein, the N terminus is still functional, indicating possible interaction of cMyBP-C^{C10mut} with actin and myosin leading to improper contraction. To support this notion, the phosphorylation level of cMyBP-C at Ser-273, Ser-282, and Ser-302 sites, which are located in the N-terminal region (M-domain) of cMyBP-C, was preserved in the cMyBP-C^{C10mut}-expressing cardiomyocytes. These data suggest that a normal level of cMyBP-C^{C10mut} phosphorylation at these sites is sufficient to regulate its dynamic interaction with actin and myosin S2 region, even though cMyBP-C^{C10mut} is not present in the C-zone. Thus, it is possible that the N-terminal of cMyBP-C^{C10mut} transiently interacts with myosin and actin in and outside the C-zone, preventing normal regulation by cMyBP-C. This could lead to contractile dysfunction because incubation of an N-terminal cMyBP-C fragment in permeabilized human myocardium caused contractile dysfunction by preventing endogenous cMyBP-C from regulating cross-bridge cycling (10). Furthermore, severe cardiac dysfunction, hypertrophy, and ultimately heart failure developed in a transgenic mouse model expressing the same N-terminal fragment (43). Part of the contractile dysfunction might be caused by changes in Ca^{2+} sensitivity of force development. N-terminal fragments have been shown to cause alterations in Ca^{2+} sensitivity, with some decreasing it (10), whereas other fragments have been shown to cause an increase (44, 45). Such a disruptive effect of cMyBP-C^{C10mut} expression on contractile function might be explained by interference with the still functional N terminus of cMyBP-C. Our studies clearly determined that 40% expression of cMyBP-C^{C10mut} is sufficient to result in contractile dysfunction.

cMyBP-C^{C10mut} Disease Mechanism—Reports in the literature suggest that cMyBP-C HCM-associated mutant proteins cause disease through poison polypeptide effects, haploinsufficiency, or ubiquitin-proteasome system impairment. Most of the truncation mutations in the C-terminal portion of cMyBP-C lead to haploinsufficiency (6), as the truncated proteins were never found in the heart (7, 8). This leads to a reduced cMyBP-C protein level, because the healthy allele can only partly compensate. If the carriers are homozygous, then C-terminally truncated mutations result in a cMyBP-C null phenotype, leading to HCM at early ages (46). In patients with the *$MYBPC3^{\Delta 25bp}$* mutation, it was reported that no mutant protein could be detected in heart tissue (19). However, this was based on protein analysis in two tissue samples and on the assumption that the mutant protein would have a different migration speed on SDS-PAGE. Because the difference in molecular mass between cMyBP-C (140,762 Da) and cMyBP-C^{C10mut} (computed molecular mass, 139,405 Da) is less than 1%, the two proteins are likely to run at the same height. In fact, in our experiments, this did happen (Fig. 2*B*). Therefore, exper-

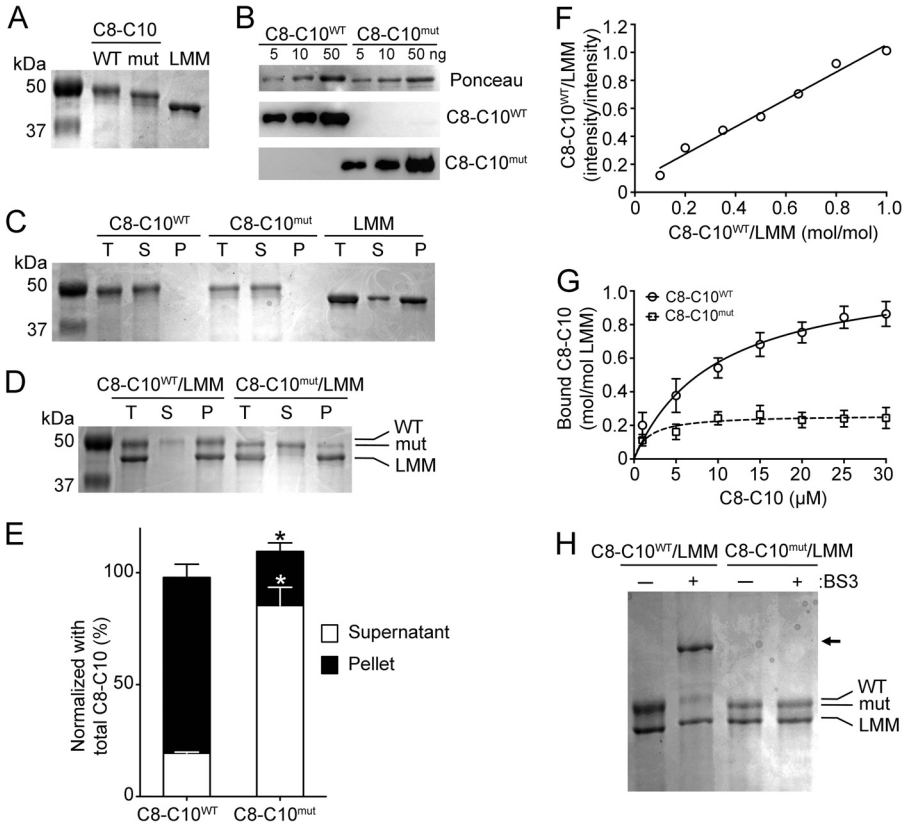

FIGURE 8. **cMyBP-C^{C10mut} has lost C10 domain interaction with myosin LMM.** *A*, SDS-PAGE analysis followed by Coomassie Blue staining demonstrated the purity of His-tagged recombinant C8-C10^{WT}, C8-C10^{mut}, and myosin LMM proteins. *B*, various concentrations of C8-C10 recombinant proteins were used to show purity using anti-C10^{WT} rabbit antibodies and anti-C10^{mut} monoclonal antibodies. Ponceau staining was used to verify equal loading on the nitrocellulose membrane. *C*, prior to the co-sedimentation assay, recombinant proteins were individually tested for their sedimentation capacity. Net protein content before centrifugation (total (*T*)) and after centrifugation in the supernatants (*S*) and pellets (*P*) was determined by SDS-PAGE and Coomassie Blue staining of the gels. *D*, co-sedimentation of either C8-C10^{WT} or C8-C10^{mut} with LMM proteins. All protein concentrations were 6 μM in the assay at 250,000 $\times$ *g* for 10 min at 4 °C. Co-sedimentation between C8-C10^{WT} and LMM indicates interaction, as illustrated by the presence of C8-C10^{WT} in the pellet, whereas C8-C10^{mut} showed little binding. *E*, quantitative data summarized the amount of C8-C10^{WT} and C8-C10^{mut} proteins in the supernatants (S) and pellets (P) after centrifugation (n = 3). *, $p < 0.001$. *F*, a representative standard curve showing a range of known molar concentrations (4–40 pmol) of C8-C10^{WT} to myosin LMM (40 pmol) on the *x* axis that were blotted against the SDS-PAGE band intensity on the *y* axis. *G*, co-sedimentation assay was performed with varying concentration (1–30 μM) of either C8-C10^{WT} or C8-C10^{mut} to 5 μM of myosin LMM to determine the K_d and B_{max} values. The K_d and B_{max} values for C8-C10^{WT} (*circles*) were of 9.8 $\pm$ 1.8 and 1.14 $\pm$ 0.08 mol/mol (n = 5, means $\pm$ S.E.). Because C8-C10^{mut} (*squares*) did not bind to myosin LMM, no significant K_d and B_{max} values could be determined (n = 5, means $\pm$ S.E.). *H*, cross-linking analysis of either C8-C10^{WT} or C8-C10^{mut} with LMM showed cross-linking of C8-C10^{WT} with LMM (*arrow*), indicating interaction, whereas C8-C10^{mut} did not cross-link to LMM. *BS3*, bis[sulfosuccinimidyl] suberate.

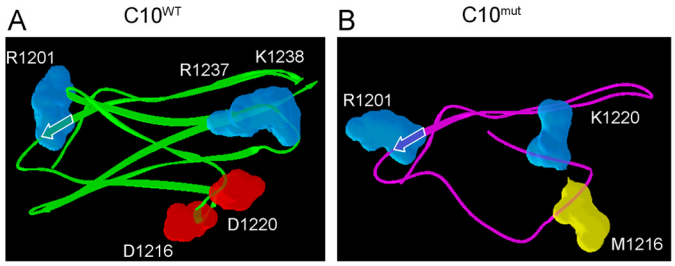

FIGURE 9. **Homology models of C10^{WT} and C10^{mut} domains.** The top scoring homology models were selected as representative structures for the C10 domains. β-Sheets are indicated by *arrows*. LMM-binding residues in C10^{WT} (*A*) are labeled. The corresponding amino acids in C10^{mut} (*B*) are labeled.

iments with mutant-specific antibodies are needed to truly determine whether and how much mutant protein is present in human myocardium.

Conversely, with missense mutations and mutations with partial modifications like cMyBP-C^{C10mut}, the mechanism of HCM disease development is entirely different. The full-length protein is expressed and either completely or partially incorporated into the sarcomere, which would then cause poison polypeptide effects that result in contractile dysfunction. Based on the results obtained from the present *in vitro* study, cMyBP-C^{C10mut} could act as such a poison polypeptide. Although cMyBP-C^{C10mut} is expressed and localized improperly, it affects contraction without changing the levels of cMyBP-C in the myofilament. This effect could be mediated by its still intact N terminus, which, if not anchored correctly into the sarcomere, would cause contractile dysfunction (10, 43).

An alternative, albeit not mutually exclusive, pathomechanism for cMyBP-C^{C10mut} could be through impairment of the ubiquitin-proteasome system (UPS). cMyBP-C mutants have been described to be targeted by the UPS (47, 48). The large supply of mutant protein can overwhelm the UPS, eventually leading to impairment of the system (47, 49). Indeed HCM patients with mutations have lower proteasome activity than patients in whom no mutation was identified (50). The impairment of the UPS may have a number of consequences that could contribute to the disease process. It could lead to an accumulation of malfunctioning proteins, including cMyBP-C. It could also lead to the formation of aggregates of unfolded pro-

teins. Because the UPS system decreases in the heart with age (51), UPS impairment could also be an explanation for the marked age-dependent increase in disease penetrance in *MYBPC3*$^{\Delta 25bp}$ mutation carriers (19).

In conclusion, we have, for the first time, shown that expression of the HCM-associated cMyBP-C^{C10mut} is sufficient to cause contractile dysfunction in cultured adult rat cardiomyocytes *in vitro*. The mutated C10 domain of the protein prevents proper localization and anchoring of the protein in the sarcomere. Further studies are in progress using both genetically engineered mouse models and human induced pluripotent stem cell-derived cardiomyocytes to define the physiology of the disease mechanism. Determining the pathogenic mechanism, which will help in developing therapeutic approaches, is the first priority to prevent the development of heart failure in millions of carriers worldwide.

REFERENCES

1. Maron, B. J., Doerer, J. J., Haas, T. S., Tierney, D. M., and Mueller, F. O. (2009) Sudden deaths in young competitive athletes: analysis of 1866 deaths in the United States, 1980–2006. *Circulation* **119,** 1085–1092
2. Alcalai, R., Planer, D., Culhaoglu, A., Osman, A., Pollak, A., and Lotan, C. (2007) Acute coronary syndrome vs nonspecific troponin elevation: clinical predictors and survival analysis. *Arch. Intern. Med.* **167,** 276–281
3. Richard, P., Charron, P., Carrier, L., Ledeuil, C., Cheav, T., Pichereau, C., Benaiche, A., Isnard, R., Dubourg, O., Burban, M., Gueffet, J. P., Millaire, A., Desnos, M., Schwartz, K., Hainque, B., and Komajda, M. (2003) Hypertrophic cardiomyopathy: distribution of disease genes, spectrum of mutations, and implications for a molecular diagnosis strategy. *Circulation* **107,** 2227–2232
4. Bonne, G., Carrier, L., Bercovici, J., Cruaud, C., Richard, P., Hainque, B., Gautel, M., Labeit, S., James, M., Beckmann, J., Weissenbach, J., Vosberg, H. P., Fiszman, M., Komajda, M., and Schwartz, K. (1995) Cardiac myosin binding protein-C gene splice acceptor site mutation is associated with familial hypertrophic cardiomyopathy. *Nat. Genet.* **11,** 438–440
5. Watkins, H., Conner, D., Thierfelder, L., Jarcho, J. A., MacRae, C., McKenna, W. J., Maron, B. J., Seidman, J. G., and Seidman, C. E. (1995) Mutations in the cardiac myosin binding protein-C gene on chromosome 11 cause familial hypertrophic cardiomyopathy. *Nat. Genet.* **11,** 434–437
6. Harris, S. P., Lyons, R. G., and Bezold, K. L. (2011) In the thick of it: HCM-causing mutations in myosin binding proteins of the thick filament. *Circ. Res.* **108,** 751–764
7. Rottbauer, W., Gautel, M., Zehelein, J., Labeit, S., Franz, W. M., Fischer, C., Vollrath, B., Mall, G., Dietz, R., Kübler, W., and Katus, H. A. (1997) Novel splice donor site mutation in the cardiac myosin binding protein-C gene in familial hypertrophic cardiomyopathy. Characterization of cardiac transcript and protein. *J. Clin. Invest.* **100,** 475–482
8. van Dijk, S. J., Dooijes, D., dos Remedios, C., Michels, M., Lamers, J. M., Winegrad, S., Schlossarek, S., Carrier, L., ten Cate, F. J., Stienen, G. J., and van der Velden, J. (2009) Cardiac myosin binding protein-C mutations and hypertrophic cardiomyopathy: haploinsufficiency, deranged phosphorylation, and cardiomyocyte dysfunction. *Circulation* **119,** 1473–1483
9. Barefield, D., and Sadayappan, S. (2010) Phosphorylation and function of cardiac myosin binding protein-C in health and disease. *J. Mol. Cell Cardiol.* **48,** 866–875
10. Witayavanitkul, N., Ait Mou, Y., Kuster, D. W., Khairallah, R. J., Sarkey, J., Govindan, S., Chen, X., Ge, Y., Rajan, S., Wieczorek, D. F., Irving, T., Westfall, M. V., de Tombe, P. P., and Sadayappan, S. (2014) Myocardial infarction-induced N-terminal fragment of cardiac myosin-binding protein C (cMyBP-C) impairs myofilament function in human myocardium. *J. Biol. Chem.* **289,** 8818–8827
11. Starr, R., and Offer, G. (1978) The interaction of C-protein with heavy meromyosin and subfragment-2. *Biochem. J.* **171,** 813–816
12. Flashman, E., Watkins, H., and Redwood, C. (2007) Localization of the binding site of the C-terminal domain of cardiac myosin binding protein-C on the myosin rod. *Biochem. J.* **401,** 97–102
13. Stelzer, J. E., Dunning, S. B., and Moss, R. L. (2006) Ablation of cardiac myosin binding protein-C accelerates stretch activation in murine skinned myocardium. *Circ. Res.* **98,** 1212–1218
14. Stelzer, J. E., Patel, J. R., Walker, J. W., and Moss, R. L. (2007) Differential roles of cardiac myosin-binding protein C and cardiac troponin I in the myofibrillar force responses to protein kinase A phosphorylation. *Circ. Res.* **101,** 503–511
15. Tong, C. W., Stelzer, J. E., Greaser, M. L., Powers, P. A., and Moss, R. L. (2008) Acceleration of crossbridge kinetics by protein kinase A phosphorylation of cardiac myosin binding protein-C modulates cardiac function. *Circ. Res.* **103,** 974–982
16. Korte, F. S., McDonald, K. S., Harris, S. P., and Moss, R. L. (2003) Loaded shortening, power output, and rate of force redevelopment are increased with knockout of cardiac myosin binding protein-C. *Circ. Res.* **93,** 752–758
17. Kuster, D. W., Sequeira, V., Najafi, A., Boontje, N. M., Wijnker, P. J., Witjas-Paalberends, E. R., Marston, S. B., Dos Remedios, C. G., Carrier, L., Demmers, J. A., Redwood, C., Sadayappan, S., and van der Velden, J. (2013) GSK3β phosphorylates newly identified site in the proline-alanine-rich region of cardiac myosin-binding protein C and alters cross-bridge cycling kinetics in human: short communication. *Circ. Res.* **112,** 633–639
18. Bardswell, S. C., Cuello, F., Kentish, J. C., and Avkiran, M. (2012) cMyBP-C as a promiscuous substrate: phosphorylation by non-PKA kinases and its potential significance. *J. Muscle Res. Cell Motil.* **33,** 53–60
19. Dhandapany, P. S., Sadayappan, S., Xue, Y., Powell, G. T., Rani, D. S., Nallari, P., Rai, T. S., Khullar, M., Soares, P., Bahl, A., Tharkan, J. M., Vaideeswar, P., Rathinavel, A., Narasimhan, C., Ayapati, D. R., Ayub, Q., Mehdi, S. Q., Oppenheimer, S., Richards, M. B., Price, A. L., Patterson, N., Reich, D., Singh, L., Tyler-Smith, C., and Thangaraj, K. (2009) A common MYBPC3 (cardiac myosin binding protein-C) variant associated with cardiomyopathies in South Asia. *Nat. Genet.* **41,** 187–191
20. Kuster, D. W., and Sadayappan, S. (2014) MYBPC3's alternate ending: consequences and therapeutic implications of a highly prevalent 25 bp deletion mutation. *Pflugers Arch.* **466,** 207–213
21. Waldmüller, S., Sakthivel, S., Saadi, A. V., Selignow, C., Rakesh, P. G., Golubenko, M., Joseph, P. K., Padmakumar, R., Richard, P., Schwartz, K., Tharakan, J. M., Rajamanickam, C., and Vosberg, H. P. (2003) Novel deletions in MYH7 and MYBPC3 identified in Indian families with familial hypertrophic cardiomyopathy. *J. Mol. Cell Cardiol.* **35,** 623–636
22. Barefield, D., Kumar, M., de Tombe, P. P., and Sadayappan, S. (2014) Contractile dysfunction in a mouse model expressing a heterozygous MYBPC3 mutation associated with hypertrophic cardiomyopathy. *Am. J. Physiol. Heart Circ. Physiol.* **306,** H807–H815
23. Sarkey, J. P., Chu, M., McShane, M., Bovo, E., Ait Mou, Y., Zima, A. V., de Tombe, P. P., Kartje, G. L., and Martin, J. L. (2011) Nogo-A knockdown inhibits hypoxia/reoxygenation-induced activation of mitochondrial-dependent apoptosis in cardiomyocytes. *J. Mol. Cell Cardiol.* **50,** 1044–1055
24. Govindan, S., Sarkey, J., Ji, X., Sundaresan, N. R., Gupta, M. P., de Tombe, P. P., and Sadayappan, S. (2012) Pathogenic properties of the N-terminal region of cardiac myosin binding protein-C in vitro. *J. Muscle Res. Cell Motil.* **33,** 17–30
25. Wilkins, M. R., Gasteiger, E., Bairoch, A., Sanchez, J. C., Williams, K. L., Appel, R. D., and Hochstrasser, D. F. (1999) Protein identification and analysis tools in the ExPASy server. *Methods Mol. Biol.* **112,** 531–552
26. Gill, S. C., and von Hippel, P. H. (1989) Calculation of protein extinction coefficients from amino acid sequence data. *Anal. Biochem.* **182,** 319–326
27. Shaffer, J. F., Kensler, R. W., and Harris, S. P. (2009) The myosin-binding protein C motif binds to F-actin in a phosphorylation-sensitive manner. *J. Biol. Chem.* **284,** 12318–12327
28. Dihazi, G. H., and Sinz, A. (2003) Mapping low-resolution three-dimensional protein structures using chemical cross-linking and Fourier transform ion-cyclotron resonance mass spectrometry. *Rapid Commun. Mass Spectrom.* **17,** 2005–2014
29. Arnold, K., Bordoli, L., Kopp, J., and Schwede, T. (2006) The SWISS-MODEL workspace: a web-based environment for protein structure homology modelling. *Bioinformatics* **22,** 195–201
30. Biasini, M., Bienert, S., Waterhouse, A., Arnold, K., Studer, G., Schmidt,

T., Kiefer, F., Cassarino, T. G., Bertoni, M., Bordoli, L., and Schwede, T. (2014) SWISS-MODEL: modelling protein tertiary and quaternary structure using evolutionary information. *Nucleic Acids Res.* **42,** W252–W258
31. Benkert, P., Tosatto, S. C., and Schomburg, D. (2008) QMEAN: A comprehensive scoring function for model quality assessment. *Proteins* **71,** 261–277
32. de Beer, T. A., Berka, K., Thornton, J. M., and Laskowski, R. A. (2014) PDBsum additions. *Nucleic Acids Res.* **42,** D292–D296
33. Gilbert, R., Kelly, M. G., Mikawa, T., and Fischman, D. A. (1996) The carboxyl terminus of myosin binding protein-C (MyBP-C, C-protein) specifies incorporation into the A-band of striated muscle. *J. Cell Sci.* **109,** 101–111
34. Miyamoto, C. A., Fischman, D. A., and Reinach, F. C. (1999) The interface between MyBP-C and myosin: site-directed mutagenesis of the CX myosin-binding domain of MyBP-C. *J. Muscle Res. Cell Motil.* **20,** 703–715
35. Freiburg, A., and Gautel, M. (1996) A molecular map of the interactions between titin and myosin binding protein-C: implications for sarcomeric assembly in familial hypertrophic cardiomyopathy. *Eur. J. Biochem.* **235,** 317–323
36. Fürst, D. O., Vinkemeier, U., and Weber, K. (1992) Mammalian skeletal muscle C-protein: purification from bovine muscle, binding to titin and the characterization of a full-length human cDNA. *J. Cell Sci.* **102,** 769–778
37. Okagaki, T., Weber, F. E., Fischman, D. A., Vaughan, K. T., Mikawa, T., and Reinach, F. C. (1993) The major myosin binding domain of skeletal muscle MyBP-C (C protein) resides in the COOH-terminal, immunoglobulin C2 motif. *J. Cell Biol.* **123,** 619–626
38. Welikson, R. E., and Fischman, D. A. (2002) The C-terminal IgI domains of myosin-binding proteins C and H (MyBP-C and MyBP-H) are both necessary and sufficient for the intracellular crosslinking of sarcomeric myosin in transfected non-muscle cells. *J. Cell Sci.* **115,** 3517–3526
39. Sadayappan, S., Gulick, J., Osinska, H., Barefield, D., Cuello, F., Avkiran, M., Lasko, V. M., Lorenz, J. N., Maillet, M., Martin, J. L., Brown, J. H., Bers, D. M., Molkentin, J. D., James, J., and Robbins, J. (2011) A critical function for Ser-282 in cardiac myosin binding protein-C phosphorylation and cardiac function. *Circ. Res.* **109,** 141–150
40. Alders, M., Jongbloed, R., Deelen, W., van den Wijngaard, A., Doevendans, P., Ten Cate, F., Regitz-Zagrosek, V., Vosberg, H. P., van Langen, I., Wilde, A., Dooijes, D., and Mannens, M. (2003) The 2373insG mutation in the MYBPC3 gene is a founder mutation, which accounts for nearly one-fourth of the HCM cases in the Netherlands. *Eur. Heart J.* **24,** 1848–1853
41. Adalsteinsdottir, B., Teekakirikul, P., Maron, B. J., Burke, M. A., Gudbjartsson, D. F., Holm, H., Stefansson, K., DePalma, S. R., Mazaika, E., McDonough, B., Danielsen, R., Seidman, J. G., Seidman, C. E., and Gunnarsson, G. T. (2014) Nationwide study on hypertrophic cardiomyopathy in iceland: evidence of a MYBPC3 founder mutation. *Circulation* **130,** 1158–1167
42. Simonson, T. S., Zhang, Y., Huff, C. D., Xing, J., Watkins, W. S., Witherspoon, D. J., Woodward, S. R., and Jorde, L. B. (2010) Limited distribution of a cardiomyopathy-associated variant in India. *Ann. Hum. Genet.* **74,** 184–188
43. Razzaque, M. A., Gupta, M., Osinska, H., Gulick, J., Blaxall, B. C., and Robbins, J. (2013) An endogenously produced fragment of cardiac myosin-binding protein C is pathogenic and can lead to heart failure. *Circ. Res.* **113,** 553–561
44. Herron, T. J., Rostkova, E., Kunst, G., Chaturvedi, R., Gautel, M., and Kentish, J. C. (2006) Activation of myocardial contraction by the N-terminal domains of myosin binding protein-C. *Circ. Res.* **98,** 1290–1298
45. Harris, S. P., Rostkova, E., Gautel, M., and Moss, R. L. (2004) Binding of myosin binding protein-C to myosin subfragment S2 affects contractility independent of a tether mechanism. *Circ. Res.* **95,** 930–936
46. Zahka, K., Kalidas, K., Simpson, M. A., Cross, H., Keller, B. B., Galambos, C., Gurtz, K., Patton, M. A., and Crosby, A. H. (2008) Homozygous mutation of MYBPC3 associated with severe infantile hypertrophic cardiomyopathy at high frequency among the Amish. *Heart* **94,** 1326–1330
47. Bahrudin, U., Morisaki, H., Morisaki, T., Ninomiya, H., Higaki, K., Nanba, E., Igawa, O., Takashima, S., Mizuta, E., Miake, J., Yamamoto, Y., Shirayoshi, Y., Kitakaze, M., Carrier, L., and Hisatome, I. (2008) Ubiquitin-proteasome system impairment caused by a missense cardiac myosin-binding protein C mutation and associated with cardiac dysfunction in hypertrophic cardiomyopathy. *J. Mol. Biol.* **384,** 896–907
48. Sarikas, A., Carrier, L., Schenke, C., Doll, D., Flavigny, J., Lindenberg, K. S., Eschenhagen, T., and Zolk, O. (2005) Impairment of the ubiquitin-proteasome system by truncated cardiac myosin binding protein C mutants. *Cardiovasc. Res.* **66,** 33–44
49. Schlossarek, S., Englmann, D. R., Sultan, K. R., Sauer, M., Eschenhagen, T., and Carrier, L. (2012) Defective proteolytic systems in Mybpc3-targeted mice with cardiac hypertrophy. *Basic Res. Cardiol.* **107,** 235
50. Predmore, J. M., Wang, P., Davis, F., Bartolone, S., Westfall, M. V., Dyke, D. B., Pagani, F., Powell, S. R., and Day, S. M. (2010) Ubiquitin proteasome dysfunction in human hypertrophic and dilated cardiomyopathies. *Circulation* **121,** 997–1004
51. Bulteau, A. L., Szweda, L. I., and Friguet, B. (2002) Age-dependent declines in proteasome activity in the heart. *Arch. Biochem. Biophys.* **397,** 298–304